Variable inter- and intra-species alkaline phosphatase activity within single cells of revived dinoflagellates

Supporting Information

Mathias Girault[1], Raffaele Siano[2], Claire Labry[2], Marie Latimier[2], Cécile Jauzein[2], Thomas Beneyton[1], Lionel Buisson[1], Yolanda Del Amo[3], Jean-Christophe Baret[1,4]

1) CNRS, Univ. Bordeaux, CRPP, UMR 5031, 33600 Pessac, France.
2) Ifremer, DYNECO, F-29280 Plouzané, France.
3) CNRS, Laboratoire d'Environnements et Paléoenvironnements Océaniques et Continentaux (EPOC), UMR 5805, 33615 Pessac, France.
4) Institut Universitaire de France, 75005 Paris, France

Corresponding authors: raffaele.siano@ifremer.fr, jean-christophe.baret@u-bordeaux.fr

Key words: Alkaline phosphatase activity, single cell, microfluidic, ELF, dinoflagellate.

Supplementary information Figure 1: Schema of the microfluidic platform setup dedicated to the alkaline phosphatase assay (APA) at the single cell level. The top left panel show the optical setup and the different devices to control the path of the droplets in the microfluidic chip. The detail of the microfluidic chip is shown on the top right panel. The photomicrographs (bottom panel) illustrated the mains steps of the APA assay performed in the microfluidic.

Supplementary information Figure 2: Fluorescence spectra of four dinoflagellate strains before and after the alkaline phosphatase assay (circles and triangles, respectively; ex: 365nm). The blue and the red dashed lines are the long and shortpass filters (470-640nm) used to block blue light and the fluorescence signal of the chlorophyll pigments captured by the camera.

Supplementary information Figure 3: Photomicrographs of the double staining labelling protocol performed on the six strains of dinoflagellates. The DAPI fluorescences are located inside the cell (i.e. nucleus) while the ELF fluorescence (green dots) is located at the surface of the dinoflagellates. Scale bars are 10µm.

Supplementary information Figure 4: Flow chart of the image processing algorithm developed in this study. The main part of the software was to efficiently detect the edge of the droplets in the brightfield image. To optimize their detections, a median filter along the x axis was used to delete the salt and pepper noises. Then, a gamma correction (0.6) was applied in order to increase the difference of intensity between the objects and the background of the image. By using a threshold of 10 in pixel intensity and a distance of 5 between two interrogation pixels, an eight directions wavelet decomposition method was processed to the image in order to detect the edge of objects. From the binary images showing the edges of objects, a flood fill algorithm was computed to fill the objects. Then, circles were detected using the Hough transform. The locations of the center of the gravity and radius of droplets were saved in an array. Then, the array including the location and radius of the droplets was used to create a series of masks which perfectly fit the droplet areas. For each mask, intensity of each pixel was summed and the results were normalized by the area of the droplet.

Supplementary information Figure 5: Kinetics of the alkaline phosphatase activity of the *Scrippsiella acuminata* and *Alexandrium minutum* strains depending on the number of day where cells are cultivated in a phosphate deplete medium.

Supplementary information Figure 6: Nitrate and phosphate concentrations in the Elorn river (Pont ar Bled and Kerigeant sampling stations, respectively).

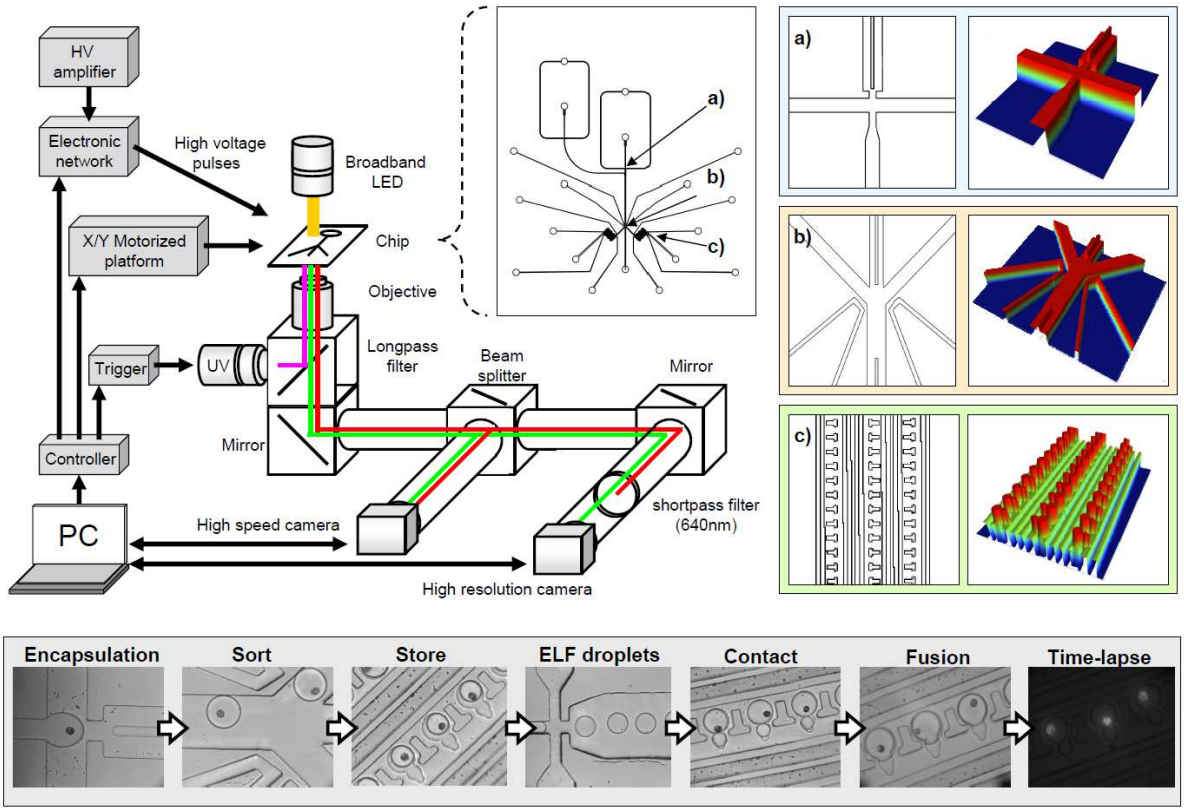

Supplementary materials Figure 1: Schema of the microfluidic platform setup dedicated to the alkaline phosphatase assay (APA) at the single cell level. The top left panel show the optical setup and the different devices to control the path of the droplets in the microfluidic chip. The detail of the microfluidic chip is shown on the top right panel. The photomicrographs (bottom panel) illustrated the mains steps of the APA assay performed in the microfluidic.

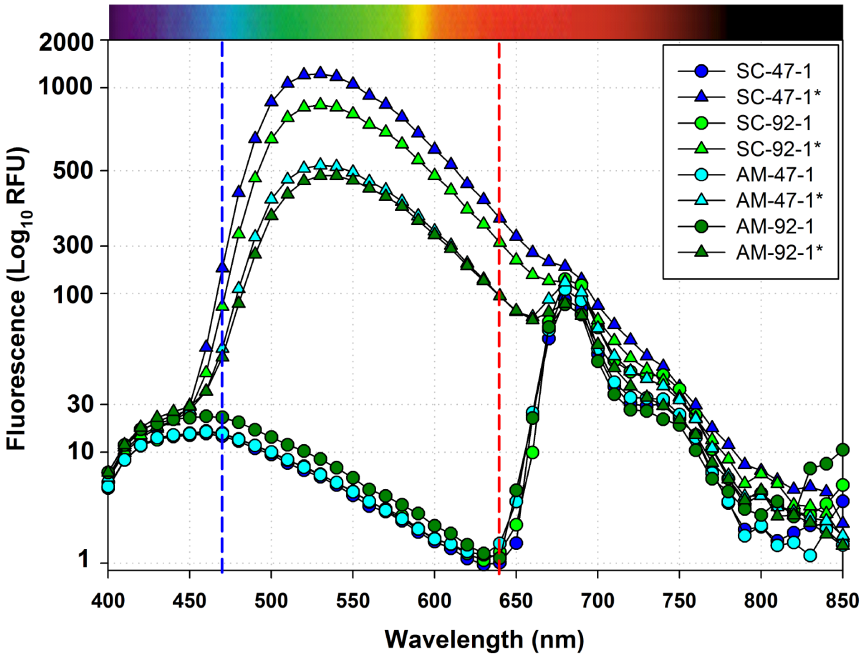

Supplementary materials Figure 2: Fluorescence spectra of four dinoflagellate strains before and after the alkaline phosphatase assay (circles and triangles, respectively; ex: 365nm). The blue and the red dashed lines are the long and shortpass filters (470-640nm) used to block blue light and the fluorescence signal of the chlorophyll pigments captured by the camera.

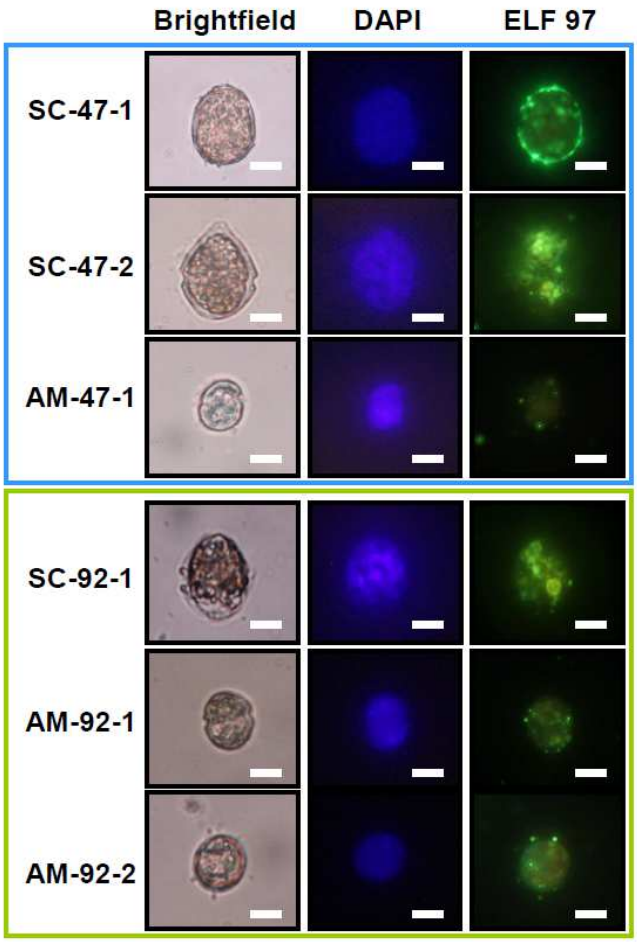

Supplementary materials Figure 3: Photomicrographs of the double staining labelling protocol performed on the six strains of dinoflagellates. The DAPI fluorescences are located inside the cell (i.e. nucleus) while the ELF fluorescence (green dots) is located at the surface of the dinoflagellates. Scale bars are 10µm.

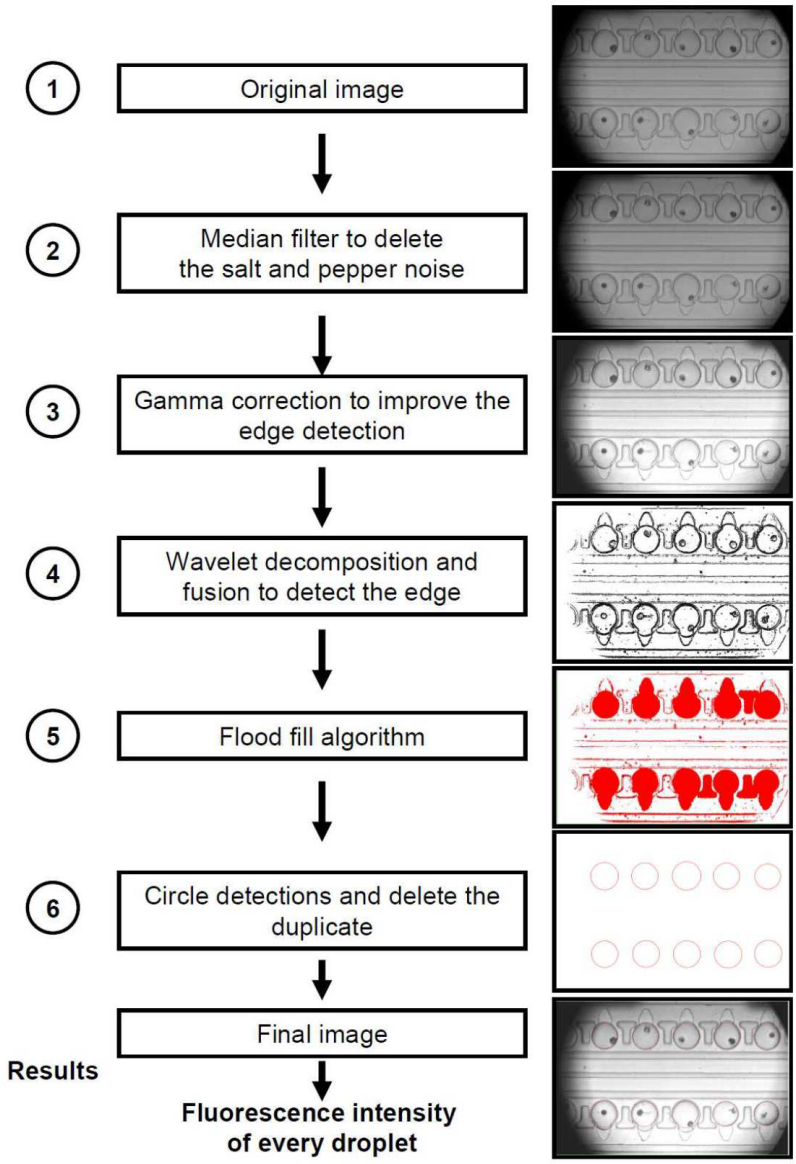

Supplementary materials Figure 4: Flow chart of the image processing algorithm developed in this study. The main part of the software was to efficiently detect the edge of the droplets in the brightfield image. To optimize their detections, a median filter along the x axis was used to delete the salt and pepper noises. Then, a gamma correction (0.6) was applied in order to increase the difference of intensity between the objects and the background of the image. By using a threshold of 10 in pixel intensity and a distance of 5 between two interrogation pixels, an eight directions wavelet decomposition method was processed to the image in order to detect the edge of objects. From the binary images showing the edges of objects, a flood fill algorithm was computed to fill the objects. Then, circles were detected using the Hough transform. The locations of the center of the gravity and radius of droplets were saved in an array. Then, the array including the location and radius of the droplets was used to create a series of masks which perfectly fit the droplet areas. For each mask, intensity of each pixel was summed and the results were normalized by the area of the droplet.

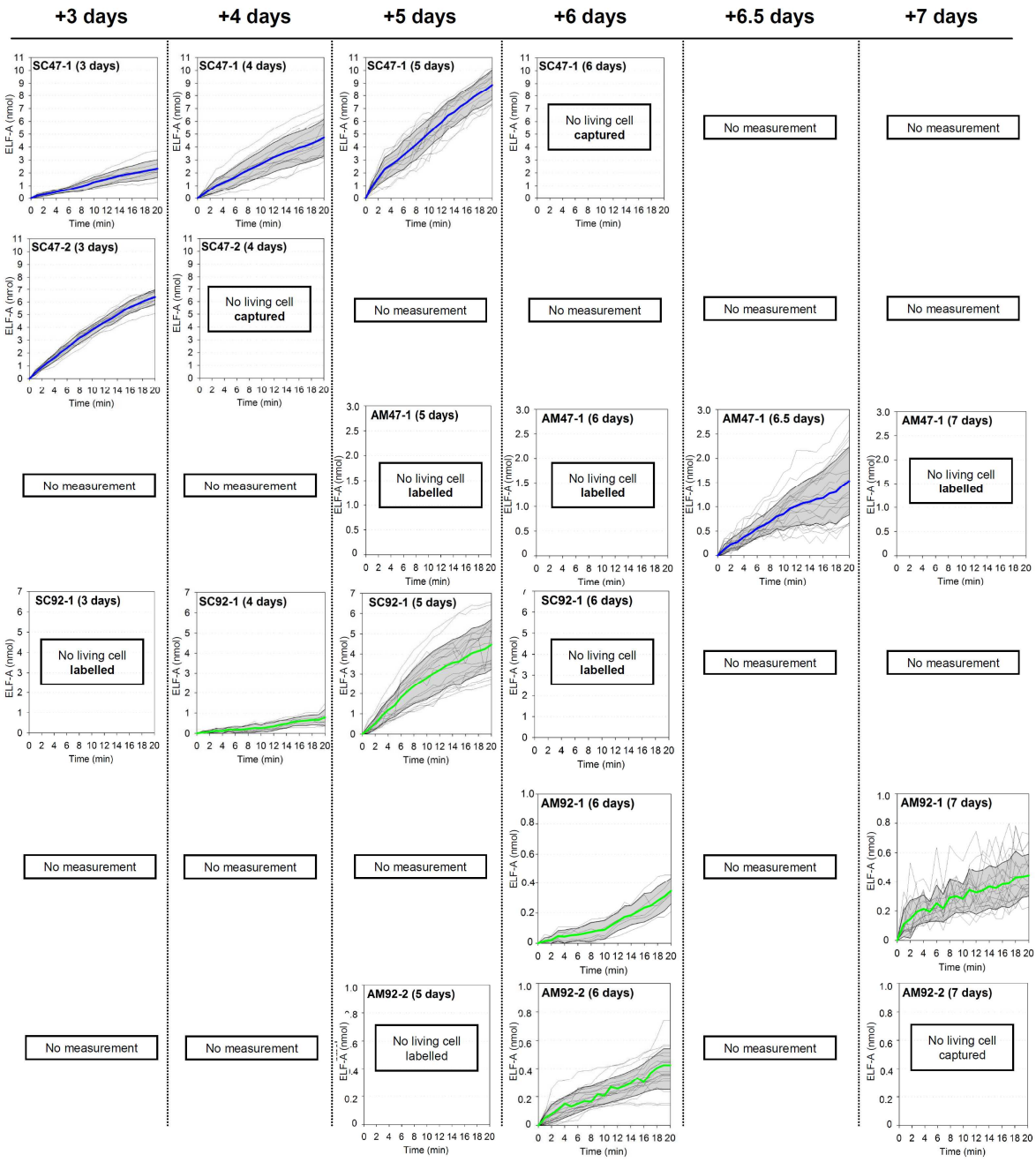

Supplementary materials Figure 5: Kinetics of the alkaline phosphatase activity of the *Scrippsiella acuminata* and *Alexandrium minutum* strains depending on the number of day where cells are cultivated in a phosphate deplete medium.

Control of the fluorescence signal during the APA assay

To test the fluorescence intensity of the natural pigments between 470nm and 640nm, an APA assay has been performed on four cultures of dinoflagellates in microtiter plate (SC-47-1; SC-92-1; AM-47-1; AM-92-1; Supplementary materials Fig. 2). As the fluorescence of the ELF-A product is located between the armour plates of the dinoflagellates, the presence of the bacteria harboured in these spaces have also been investigated in the cultures. A double staining protocol (4′,6-diamidino-2-phenylindole DAPI and ELF) was assayed when the cell expressed the APA. The results indicated that only the nucleus of the dinoflagellate is stained by the DAPI (Supplementary materials Fig. 3). The absence of DAPI product at the same location as the ELF showed that bacteria were not responsible for the fluorescence of the ELF in the samples. Finally, to minimize the exposure time of cells to the harmful short wavelength, the ultraviolet LED was connected to a diaphragm shutter with a controller (SHB1T, Thorlabs). Typically, an exposition of 500 ms every 2 min was observed to not induce lyses of cells and not significantly bleach the intensity of the fluorescent product (*i.e*. ELF-A)

Historical nutrient data in the Bay of Brest

The Bay of Brest is a semi-enclosed basin fertilized by two main rivers (Aulne and Elorn) and waste-waters from human activities. According to the location of the sediment core used in this study, the hydrology of the Elorn river was considered in order to describe the changes of the environmental conditions. At the end of WWII, the industry and agriculture were particularly weakened by years of wars. Under these circumstances, nitrate and phosphate loads to the Bay through riverine inputs were probably particularly low. Because of the important circulation in the Bay of Brest (driven by tidal movement and residual currents) nutrient accumulation is limited (the residence time of seawater ranged from 3 days to 1 month; [85-86]. From the end of the WWII, a broad period of worldwide economic expansion, mainly initiated by the Marshall and Monnet plans tended to modernize both the industry and agriculture in France. Within this new context, the use of fertilizers (mainly nitrate and in a lesser extent phosphate) was largely promoted and used from the 1960's in order to increase the agricultural yield. Due in part to the high affinity of nitrate to leach from the soil, the nitrate inputs from the rivers strongly fertilized the roadstead of Brest. For example, one of the first studies conducted after the WWII pointed out that nitrate concentration in the estuary of Elorn river in the winters 1979-1981 was particularly high (400 $\mu mol.L^{-1}$; same order as the Seine river; a major river near Paris metropole, France) and nitrate charge in summer was so high that the phytoplankton growth in the estuary did not significantly decrease the nitrate concentration in summer [87, 88]. At the end of the 1970's, the growth of phytoplankton was strongly correlated to the nutrient pulses from rivers where several phytoplankton blooms were observed within the same year [89]. In the early 1980's, the ratio N/P reached 30 (*i.e.* >16 Redfield ratio) before the spring bloom of phytoplankton but the main limiting factor for phytoplankton was still reported to be the nitrate [89, 90]. From the early 1980's to the 1990's, the N/P ratio keeps increasing because of the long delay in efficiently regulating nitrate in agriculture together with the laws which severely limited phosphate discharges from anthropogenic activities (European directive 91/271, May 21st 1991; CJEU June 13th 2013: 62012CJ0193). As a consequence, the 1990's decade was characterized by the highest nitrate concentrations ever measured in the Elorn river (annual average is 613µM in 1992 and up to 667µM in 1993, Supplementary materials Fig. 6). In the same decade, phosphate concentrations in the Elorn river ranged from 1.4 µM to 3.6 µM leading to N/P ratios spread from 170 to 426 (Supplementary materials, Fig. 6). Despite the potential increase of phosphate concentrations within the bay waters from 1947 to 1992, these values indicated that the inputs of nutrients in the Bay of Brest were progressively unbalanced in relation to the higher nitrate concentrations. A possible visible consequence was that diatom blooms observed in 1993 and 1994 appeared to be firstly Si- and P-limited and then, in the lesser extend N-limited within the productive period from spring to summer [91]. Fifteen years before, N was the main limiting factor for phytoplankton in the Bay of Brest [92].

85 C. Francis-Bœuf, Les phénomènes de sédimentation dans les estuaires, Bulletin de l'association de Géographes Français. 1942;146-147,64–78.

86 P. Bassoulet, Etude de la dynamique des sédiments en suspension dans l'estuaire de l'Aulne (Rade de Brest). 1979, PhD, UBO, Brest, pp. 136.

87 R. Delmas, Etude de l'évolution saisonnière des sels nutritifs dans la rade de Brest en fonction des apports fluviaux et des échanges avec l'iroise. PhD, University de Bretagne occidentale. 1981, pp163. https://archimer.ifremer.fr/doc/00103/21454.

88 R. Delmas, P. Tréguer, Seasonal variation of nutrients in an eutrophie ecosystem of Western Europe (Bay of Brest). Marine and terrestrial interactions. *Oceanol. Acta*. 6, 345–356 (1983).

89 D. Delmas, M. Hafsaoui, S. Le Jehan, B. Quéguiner, P. Tréguer, Effect of large seasonal and annual variable fertilizations on phytoplankton in an eutrophic ecosystem. *Oceanol. Acta*. 1983. Proceedings 17th European Marine Biology Symposium, Brest, France, 27th Sept.-1st Oct, 1982, 81–85.

90 R. Geider, J. La Roche, Redfield revisited: variability of C:N:P in marine microalgae and its biochemical basis. *Eur. J. Phycol.* 37, 1–17 (2002).

91 Y. Del Amo, O. Le Pape, P. Treguer, B. Queguiner, A. Menesguen, A. Aminot, Impacts of high-nitrate freshwater inputs on macrotidal ecosystems. I. Seasonal evolution of nutrient limitation for the diatom-dominated phytoplankton of the Bay of Brest (France). *Mar. Ecol. Prog. Ser.* 161, 213–224 (1997).

92 B. Queguiner, P. Treguer, Studies on the phytoplankton In the Bay of Brest (Western Europe). Seasonal variation in composition biomass and production in elation to hydrological and chemical features (1981-1982). *Bot. Mar.* 27, 449–459 (1984).

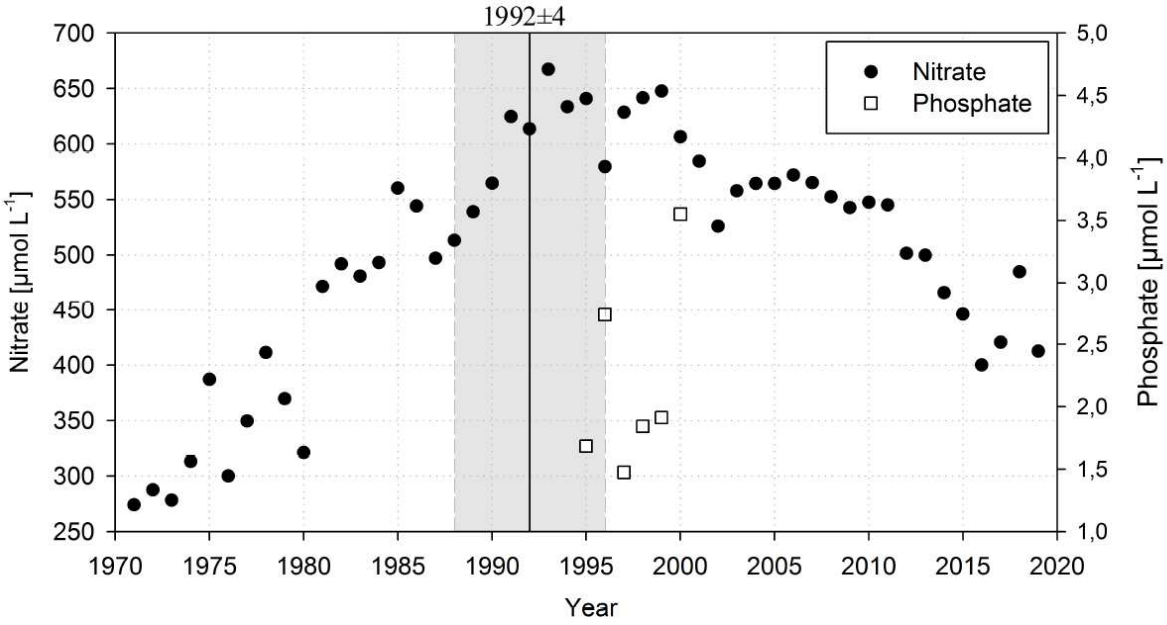

Supplementary materials Figure 6: Nitrate and phosphate concentrations in the Elorn river (Pont ar Bled and Kerigeant sampling stations, respectively).